

Nuclear magnetic resonance imaging of an operating gas–liquid–solid catalytic fixed bed reactor

Anna A. Lysova^{a,*}, Igor V. Koptuyug^a, Alexander V. Kulikov^{b,1},
Valery A. Kirillov^{b,1}, Renad Z. Sagdeev^a, Valentin N. Parmon^{b,1}

^a International Tomography Center, SB RAS, 3A Institutskaya St., Novosibirsk 630090, Russia

^b Borekov Institute of Catalysis, SB RAS, 5 Acad. Lavrentiev St., Novosibirsk 630090, Russia

Abstract

This work reports our pioneering application of the nuclear magnetic resonance imaging (MRI) technique to the dynamic *in situ* studies of gas–liquid–solid reactions carried out in a catalytic trickle bed reactor at elevated temperature. The major advance of these studies is that MRI experiments are performed under reactive conditions. We have applied MRI to map the distribution of liquid phase inside a catalyst pellet as well as in a catalyst bed in an operating trickle-bed reactor. In particular, our studies have revealed the existence of the oscillating regimes of the heterogeneous catalytic hydrogenation reaction caused by the oscillations of the catalyst temperature and directly demonstrated the existence of the coupling of mass and heat transport and phase transitions with chemical reaction. The existence of the partially wetted pellets in a catalyst bed which are potentially responsible for the appearance of hot spots in the reactor has been also visualized. The combination of NMR spectroscopy with MRI has been used to visualize the spatial distribution of the reactant-to-product conversion within an operating reactor.

© 2006 Elsevier B.V. All rights reserved.

Keywords: Nuclear magnetic resonance imaging; Multiphase catalytic reactions; Hot spots formation; NMR spectroscopy with spatial resolution

1. Introduction

The sophisticated nature of image contrast in nuclear magnetic resonance imaging (MRI) makes it one of the most powerful tomographic techniques available at present [1–3]. In principle, the MRI toolkit can characterize all essential aspects related to structure, transport and behavior of an operating reactor (spatial distribution and flow fields of liquids and gases, structure of the solid phase, heat transport, spatially resolved distribution of the reactants and products). But until now the potential of MRI in the field of reaction engineering remains practically unexplored. Most of the MRI studies of chemical reactions performed hitherto were carried out in a homogeneous medium and/or at room temperature.

This work reports our pioneering application of the MRI technique to the dynamic *in situ* studies of gas–liquid–solid reactions carried out in a catalytic trickle bed reactor at elevated temperatures, with the spatial resolution high enough to monitor

processes within individual catalyst pellets comprising the granular bed. A reaction of a heterogeneous catalytic hydrogenation of α -methylstyrene (AMS) has been chosen for this study for its practical importance in chemical industry. The major advance of these studies is that MRI experiments are performed under reactive conditions.

2. Experimental

All MRI experiments were carried out on an Avance DRX 300 NMR spectrometer (Bruker) equipped with a vertical bore superconducting magnet and the accessories to perform the imaging experiments. ^1H NMR signal of a liquid phase at the frequency of 299.13 or 300.13 MHz was detected in the experiments. A radio-frequency coil of 25 mm inside diameter was used. To perform the experiments of catalytic hydrogenation, we built a special set-up consisting of a model reactor which can be placed directly inside the MRI probe, a system to supply hydrogen and liquid AMS, accessories to control and to measure the temperature, air heaters which provide the thermostating of the reactor, the heating of liquid AMS before its supply to the reactor and the required temperature in the saturator.

* Corresponding author. Tel.: +7 383 3333561; fax: +7 383 3333561.

E-mail addresses: lysova@tomo.nsc.ru (A.A. Lysova),

parmon@catalysis.nsk.su (V.N. Parmon).

¹ Tel.: +7 383 3308269; fax: +7 383 3308269.

The reactor that can be inserted into the magnet is an evacuated double-walled glass dewar (item (6) in Fig. 1; 25 mm outside diameter, 16 mm inside diameter, about 600 mm long). Its upper part extends about 150 mm above the upper edge of the rf coil (3) where it is connected to a single-walled glass pipe (10). The latter extends above the upper edge of the magnet and is surrounded with a wider polyfoam tube (1) to protect the upper part of the magnet bore. The dewar prevents the overheating of the gradient coils of the MRI instrument which can be easily destroyed by heating above $\sim 50^{\circ}\text{C}$. The lower end of the dewar (6) protrudes from the probe body (5) at the bottom of the magnet. To achieve this, the original 25 mm birdcage rf coil (3) (Bruker) was used in combination with a home-built Teflon probe body (5) to provide a 25 mm bore throughout the entire probe. A 10 mm inside diameter glass tube (8) is inserted concentrically in the dewar (14 mm outside diameter, 1.5 m long). The annular space between the tube (8) and the dewar (6) carries the flow of hot air for thermostating the reaction volume.

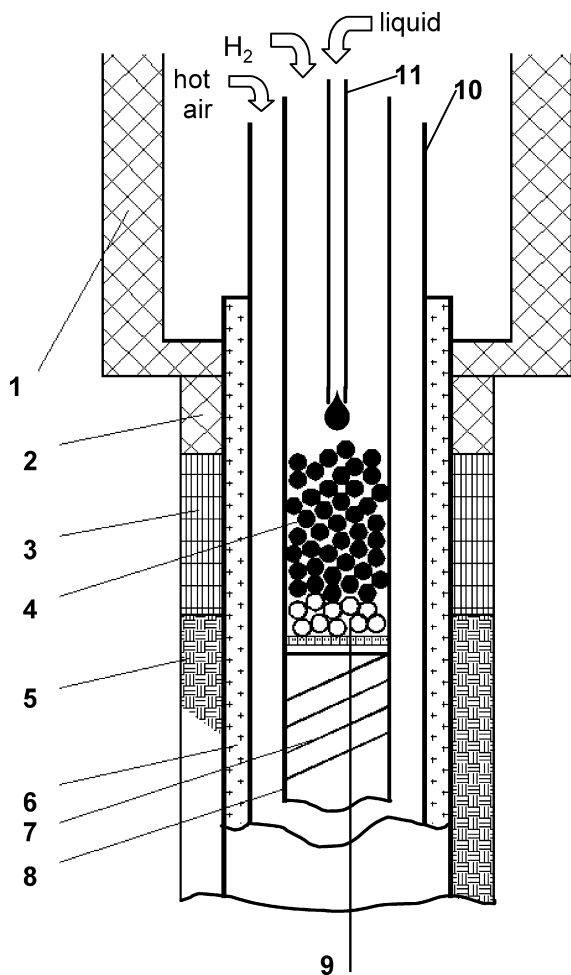


Fig. 1. Schematic drawing of the NMR-compatible multiphase catalytic reactor for MRI studies at elevated temperatures: (1) polyfoam tube; (2) Teflon holder which connects 1 with dewar 6; (3) rf coil; (4) granular catalyst bed supported by a stainless steel mesh; (5) probe body; (6) evacuated double-walled glass dewar; (7) supporting stainless steel spiral; (8) glass tube; (9) thermocouple; (10) single-walled glass pipe connected to the dewar; (11) stainless steel capillary for liquid reactant supply. The reactor is not drawn to scale, only the central part is shown.

The inner tube (8) is used to place a catalyst pellet/bed and to supply the pre-heated flow of hydrogen or mixture of hydrogen and AMS vapor. The mixture of hydrogen and AMS vapor is prepared by a preliminary saturation of hydrogen with a reagent vapor in the saturator at the temperature slightly higher than the temperature in the reactor. The temperature of the gas flow T_0 is measured with a thermocouple placed 8 mm upstream of the catalyst pellet/bed. The pellet is suspended in the inner tube by the use of a thermocouple 0.2 mm in diameter which is implanted into the pellet through its side (not shown). The thermocouple measures the temperature T_1 in the pellet center during the experiment. The vertical axis of the pellet coincides with the direction of the constant magnetic field of the superconducting magnet of the MRI instrument. The catalyst bed (4) is placed in the reactor on the layer of inert pellets of the same size which in turn is positioned on a stainless steel mesh. A stainless steel mesh is supported with a spiral (7) wound of stainless steel wire which fits tightly into the reactor tube and is inserted from the bottom together with the mesh and the thermocouple (9). Liquid AMS is supplied to the top center of the pellet/bed via a copper capillary (11) with the inner diameter of 0.2 mm. For high liquid flow rates, it was found necessary to preheat liquid AMS before its supply to the reactor to avoid a heat loss in the reaction zone. Another thermocouple measures the temperature of liquid AMS in the capillary before its supply to the bed. Two additional thermocouples are used for safety reasons, one monitors the temperature at the outer wall of the evacuated dewar while another is located in the region between the rf probe and the gradient coils.

The cylindrical catalyst pellets of 1% Pd/ $\gamma\text{-Al}_2\text{O}_3$ with the diameter of 4.5 mm and height of 12 mm were used for AMS hydrogenation on an individual catalyst pellet. The spherical catalyst pellets of 1% Pd/ $\gamma\text{-Al}_2\text{O}_3$ of 1, 2–3 and 4.2 mm in diameter were used for AMS hydrogenation in the catalyst bed. All catalyst pellets contained 0.1% Mn. Manganese was not catalytically active in the AMS hydrogenation but allowed us to decrease the repetition time of the MRI sequence and therefore the acquisition time of a two-dimensional (2D) image. The $\gamma\text{-Al}_2\text{O}_3$ pellets of 1, 2–3 and 4.2 mm in diameter also containing 0.1% Mn were used as an inert support.

Before any hydrogenation experiment, the beds of 1 and 2–3 mm pellets were activated during half an hour in a H_2 stream at 450°C , then cooled to room temperature in a He stream. The beds of 4.2 mm pellets as well as the individual catalyst pellets were activated before any hydrogenation experiment in a mixed H_2 -air stream with excess of hydrogen (catalytic hydrogen combustion), then heated to 450°C in a He stream and cooled to room temperature without interrupting a He stream.

After activation, the catalyst was placed in the reactor located in the NMR magnet. After that, a liquid reagent was supplied to the pellet/bed, the probe was tuned/matched, the parameters of the pulse and gradient sequences as well as the exact position of the catalyst in the reactor were determined. Then, depending on the type of experiments planned, either hydrogen and a liquid reagent were supplied to the reactor, or the catalyst was first dried with a stream of H_2 or He and then the reagent supplies to the reactor were turned on.

In all imaging experiments a two-pulse spin–echo sequence ($90^\circ-\tau-180^\circ-\tau$ -echo) with a 2 mm thick axial or transverse slice selection was used to obtain 2D images of a liquid phase distribution in the catalyst pellet/bed. In some experiments several transverse images of the bed off-centered relatively to the iso-center of the gradient coils were detected by shifting the transmitter frequency. Spatial information was frequency encoded in one dimension and phase encoded in the other one, with the data matrix size of (128×64) complex data points. The axial images of an individual catalyst pellet and the transverse images of the catalyst bed were obtained with $(140 \mu\text{m} \times 230 \mu\text{m})$ spatial resolution and $(1.8 \text{ cm} \times 1.5 \text{ cm})$ field of view. The number of accumulations NA was 2, the echo time TE was about 1 ms. The repetition time TR was 250 ms, resulting in the image acquisition time TA of 34 s.

Spatially resolved spectroscopic studies have been performed with a $(128 \times 16 \times 64)$ data matrix, $(2.1 \text{ cm} \times 4.2 \text{ cm})$ field of view, NA=4, TR=300 ms, TE=2.1 ms, $(1.3 \text{ mm} \times 0.66 \text{ mm})$ spatial resolution, a 2 mm thick slice and pure phase encoding of the image. The second half of the echo signal in the absence of any applied gradients was detected. The spectrum width was 25 ppm. The total experiment time was 22.5 min.

3. Results and discussion

3.1. AMS hydrogenation on an individual catalyst pellet

The experiments carried out on an individual catalyst pellet [4] have shown the formation inside the catalyst pellet of strong gradients of the liquid phase content during the impregnation of the porous catalyst with a liquid reagent under conditions of simultaneous endothermic reagent evaporation and exothermic hydrogenation of its vapor. The visualization of the liquid phase distribution inside the catalyst pellet in the course of AMS hydrogenation has revealed the existence of two zones, inside the pellet, strongly differing in the liquid phase content: the upper part filled with a liquid phase and the lower part, dry and filled with vapor, in which a vapor-phase hydrogenation occurs. A non-uniformity of the liquid phase distribution inside the catalyst pellet in the course of the reaction that has been for the first time experimentally observed by MRI can be one of the reasons of the appearance of critical phenomena on an individual catalyst pellet as well as in the catalyst bed. At the same time, for the safe operation of the catalytic reactors resulting in a good productivity it is necessary to have an optimal ratio of the wetted and dry parts of the catalyst pellet which provides the efficient heat removal via a liquid

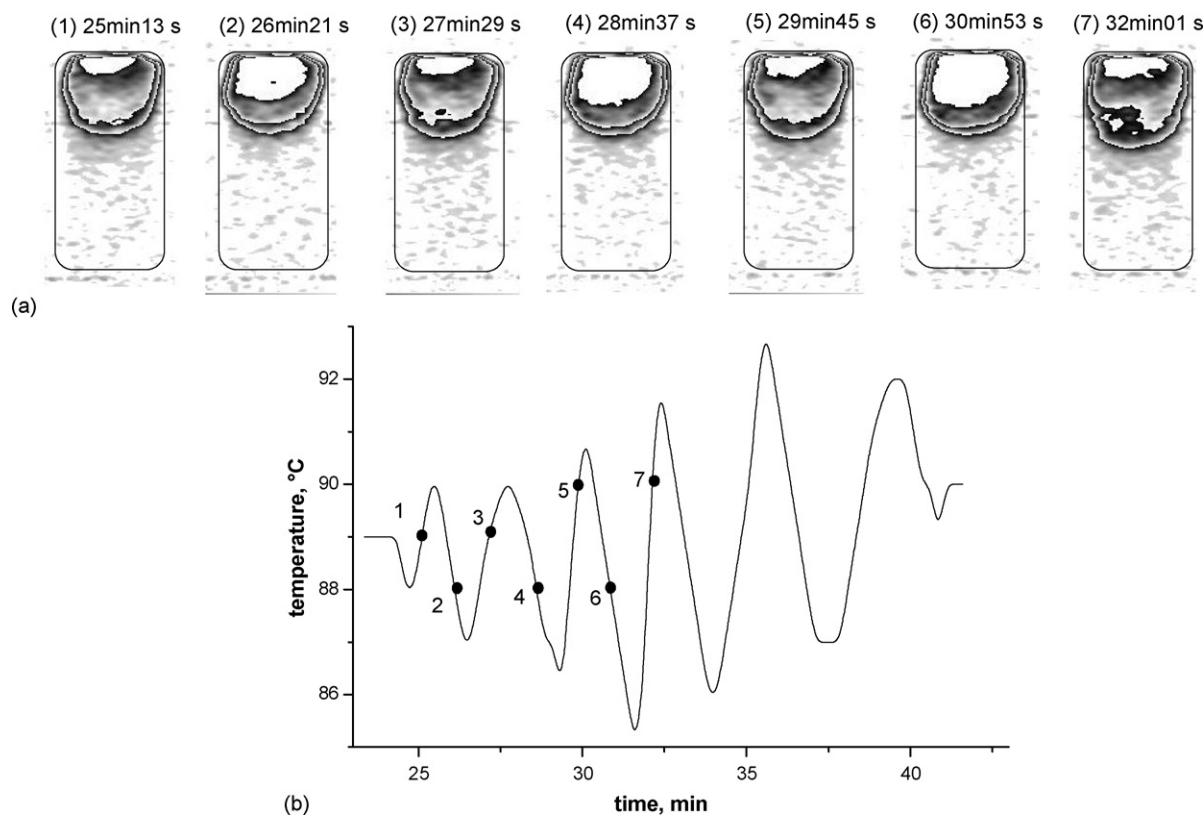


Fig. 2. (a) 2D images of the liquid phase distribution inside the catalyst pellet in the course of AMS hydrogenation under conditions of simultaneous supply of liquid AMS and hydrogen to the pellet. The intensity scale is ambiguous and was selected to improve the image contrast. The experimental conditions are presented in the text. Time corresponding to the middle of the acquisition period is shown in each image. (b) Temporal dependence of the temperature of the catalyst pellet measured in the lower part of the pellet by a thermocouple. Black points correspond to the moments when the images shown in (a) have been detected.

phase and the intense hydrogenation reaction in the gaseous phase.

Our studies have also revealed the existence of the non-stationary regime of the catalyst pellet operation in which oscillations of the liquid phase content inside the catalyst pellet and oscillations of the liquid front propagation into the porous structure have been observed. Note that the oscillatory behavior of the catalyst pellet operation has been detected under constant experimental conditions: the rate of a liquid AMS supply was 8.6×10^{-4} g/s; the rate of a hydrogen flow heated to 78 °C was 10.9 cm³/s.

The experiments carried out allow us to conclude that two types of oscillations are observed in the catalyst pellet. The 2D images representing the first type of oscillations of the liquid phase content inside the catalyst pellet are shown in Fig. 2a. The signal intensity scale of the images was intentionally made ambiguous, providing contour lines of the liquid distribution to stress the pulsating motion of the liquid front. The highest liquid content is observed in the top part of the pellet, and the size of this region and the position of its boundary exhibit unceasing pulsations. The rest of the pellet is dry and is filled with vapor–gas mixture. In the case presented in Fig. 2a a liquid phase fills the porous structure like a motion of a plunger. So, these oscillations can be called the “axial” oscillations. The oscillations of the liquid phase content were accompanied by the temperature oscillations measured by a thermocouple implanted in the lower part of the pellet (Fig. 2b). The reciprocating motion of a liquid front and the temperature oscillations were bound with the differences in the rates of AMS evaporation and an exothermic hydrogenation reaction. The temporal shift between the moments of achievement of the highest temperature value and the minimum volume of the wetted zone as well as between the moments of achievement of the lowest temperature value and the maximum volume of the wetted zone has been observed. So, the highest temperature has been achieved when the catalyst pellet has undergone the transition from the condition characterized by the minimum value of the liquid phase content to the condition characterized by the maximum value of the liquid phase content (images 1 and 2; 3 and 4; 5 and 6). The lowest temperature has been observed when the liquid phase content in the catalyst pellet has changed from the maximum value to the minimum value (images 2 and 3; 4 and 5; 6 and 7). Thus, between the pellet temperature and the amount of a liquid phase in the porous structure, a feedback with delay exists. The oscillations presented in Fig. 2 have been observed when less than a half of the catalyst pellet was filled with a liquid phase.

The peculiarity of the second type of oscillations was the propagation of a liquid phase into the porous structure to the greater depth and the existence of the essential non-uniformity of the radial liquid phase distribution in the catalyst pellet. These oscillations were also characterized by a greater amplitude of the temperature change and have reminded the grain ignition because the liquid phase content inside the pellet changed dramatically in the course of oscillations. We have called these oscillations the “radial” oscillations because, in contrast to the type of oscillations described above, they were characterized by the oscillatory motion of a liquid phase along the radius of

the pellet but not along its vertical axis. These oscillations were observed in the case when more than a half of the porous structure of the pellet was filled with a liquid phase.

The existence of oscillations of the liquid phase content on an individual catalyst pellet accompanied by the temperature oscillations can be explained on the basis of the mechanism of a delayed negative feedback. If in the case of a random disturbance the rate of a heat production due to the reaction has increased the rate of a heat removal via a liquid phase, the catalyst temperature starts to rise. This results in an increase of the pressure of the saturated vapor inside the porous structure of the pellet due to an increase of the evaporation rate and, therefore, a decrease of the liquid phase content inside the pellet and the evaporation surface area. A consequence of these processes is a deceleration with some delay of the evaporation rate resulting in a decrease of the AMS vapor pressure and the reaction rate which in turn leads to a decrease of the heat production rate. This leads to a decrease of the catalyst pellet temperature and a beginning of a new oscillatory cycle. The results obtained indicate that the differences in the rates of the heat and mass transfer processes and phase transitions are responsible for the observed oscillatory behavior of the catalyst pellet and directly demonstrate the existence of the coupling of mass and heat transport and phase transitions with the chemical reaction.

3.2. AMS hydrogenation in the catalyst bed

The character of the liquid phase distribution in the trickle bed in the course of AMS hydrogenation in various regimes of the reagent supplies has been also studied. Fig. 3 shows 2D images of the liquid phase distribution in the catalyst bed consisting of pellets of 1 mm in diameter under conditions of supply to the bed of hydrogen heated to 71 °C with a flow rate of 10.9 cm³/s. In this experiment the NMR signal intensity of a liquid phase in an axial slice of 2 mm thickness has been detected. Light grey color of the images corresponds to the higher NMR signal intensity in the regions of the higher liquid phase content, and vice versa. At the same time, zones, where the signal intensity is lower than the noise, have white color of the background of the image. The rate of a liquid AMS supply was varied in the course of the experiment. It has been revealed that a decrease or an increase of the rate of a liquid reagent supply leads correspondingly to a decrease or an increase of the liquid phase content in the catalyst bed (images 1 and 2; 6 and 7; 9 and 10 in Fig. 3), but under constant experimental conditions the catalyst bed operates in the stationary regime characterized by the constancy of the liquid phase distribution in the catalyst bed and the temperature of the bed.

In the experiment presented in Fig. 4 the catalyst pellets of 2–3 mm in diameter have been used. The catalyst bed of 3 cm height was placed on the 2 cm high inert bed. The NMR signal intensity of a liquid phase in an axial slice of 2 mm thickness has been detected during the experiment. The intensity scale is the same as in Fig. 3. The composition of a liquid phase at the outlet of a reactor was analyzed via a gas chromatography method and the results of a gas chromatographic analysis of a reaction mixture under various conditions of the reagent sup-

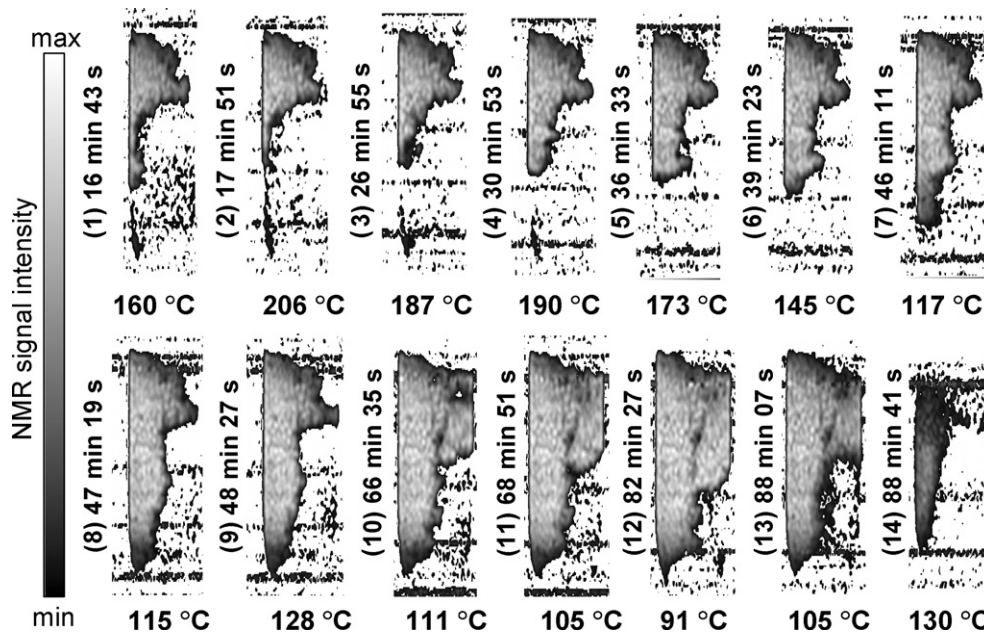


Fig. 3. 2D images of the liquid phase distribution in the catalyst bed of 1 mm 1% Pd/ γ -Al₂O₃ pellets in the course of AMS hydrogenation. The rate of liquid AMS supply was: (1) 1.95×10^{-2} g/s; (2–6) 9.71×10^{-3} g/s; (7–9) 6.64×10^{-2} g/s; (10–12) 9.36×10^{-2} g/s; (13–14) 0. Time corresponding to the middle of the acquisition period as well as the temperature of the catalyst bed at this moment is shown in each image. The change of the image intensity from dark grey to light grey corresponds to the increase of the liquid phase content, whereas in the zones of white color the NMR signal intensity is lower than the noise level.

plies are presented in Table 1. It can be seen in Fig. 4 that the liquid phase distribution in the catalyst bed and in the inert bed is practically the same but in the inert bed the zones of the NMR signal of the low intensity exist that is likely to be bound with the presence of absorbed vapor in the porous medium. Absorbed vapor is absent in the catalyst bed because of its higher temperature due to the occurrence of an exothermic reaction. It has been shown that an increase or a decrease of the rate of liquid AMS supply slightly influences the liquid phase content in

the catalyst bed but leads to an increase or a decrease of the liquid phase content in the inert bed (images 1 and 2; 3 and 5; 5 and 7 in Fig. 4). A decrease of the rate of hydrogen flow also does not change the liquid phase distribution in the catalyst bed but results in an increase of the liquid phase content in the inert bed (images 11–14 in Fig. 4). It is worth to mention that the AMS conversion also did not change when the rate of hydrogen flow was varied (Table 1). Evidently it is bound with that fact that even when the rate of the hydrogen flow was

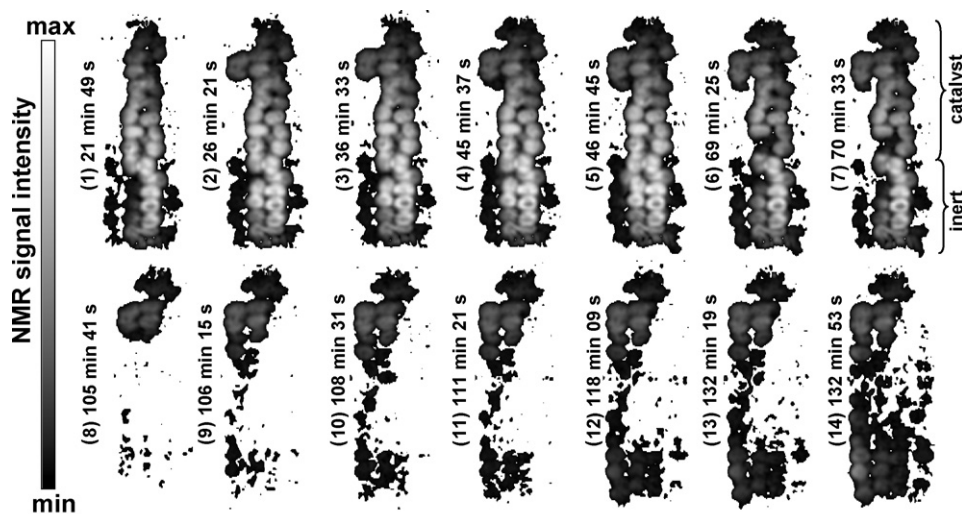


Fig. 4. 2D images of the liquid phase distribution in the catalyst bed of 2–3 mm 1% Pd/ γ -Al₂O₃ pellets in the course of AMS hydrogenation. Temperature of hydrogen flow was 85 °C. At the rate of H₂ flow of 40 cm³/s the rate of a liquid AMS supply was: (1) 5.06×10^{-2} g/s; (2, 3) 9.96×10^{-2} g/s; (4, 5) 1.47×10^{-1} g/s; (6, 7) 2.96×10^{-2} g/s; (8–10) 2.96×10^{-2} g/s (but liquid AMS was turned on to the dry bed, in contrast to the previous two images). At the rate of liquid AMS supply of 3.24×10^{-2} g/s the rate of hydrogen flow was: (11) 40 cm³/s, (12, 13) 20 cm³/s, (14) 7.9 cm³/s. Time corresponding to the middle of the acquisition period is shown in each image. The change of the image intensity from dark grey to light grey corresponds to the increase of the liquid phase content, whereas in the zones of white color the NMR signal intensity is lower than the noise level.

Table 1

Productivity of the catalyst bed consisting of 2–3 mm in diameter 1% Pd/ γ -Al₂O₃ pellets at various regimes of the reagent supply

Regime	Liquid AMS supply (g/s)	H ₂ supply (cm ³ /s)	Conversion (%)	Productivity (g/s)
1	5.06×10^{-2}	40	20.77	1.05×10^{-2}
2	9.96×10^{-2}	40	10.02	9.98×10^{-3}
3	1.47×10^{-1}	40	5.53	8.13×10^{-3}
4	2.96×10^{-2}	40	33.49	9.91×10^{-3}
5	3.24×10^{-2}	20	27.18	8.81×10^{-3}
6	3.24×10^{-2}	7.9	27.64	8.96×10^{-3}

decreased to 7.9 cm³/s, H₂ was in excess in relation to AMS and the reaction was limited by the AMS supply into the gaseous phase. Therefore, the change of the rate of hydrogen flow slightly influences the liquid phase distribution in the catalyst bed and the reagent conversion. The liquid phase content in the inert bed must be dependent on the rate of a flow of hot hydrogen because the higher the flow velocity, the more AMS can evaporate into the gaseous phase and be taken away by the hydrogen flow leading to a decrease of the liquid phase content in the inert bed.

The results of a comparison of the response of the liquid phase distribution in the catalyst bed and in the inert bed on the variation of the rates of the reagent supplies show a significant

influence of the occurrence of a reaction on the mass transfer processes in the catalyst bed.

It has been also established that the liquid phase distribution in the catalyst bed depends on the conditions of a reactor start-up. Thus, when the rate of a liquid AMS supply has been decreased from 1.47×10^{-1} to 2.96×10^{-2} g/s (images 4–7 in Fig. 4), the liquid phase content in the catalyst bed has changed slightly, and the catalyst bed turned out to be essentially filled with a liquid phase. When the liquid AMS supply with the same flow rate (2.96×10^{-2} g/s) has been turned on to the dry catalyst bed (images 8–10 in Fig. 4), the liquid phase distribution in the catalyst bed has changed dramatically in comparison to the case when the hydrogenation process was started from the bed initially filled with a liquid phase. Thus, *in situ* MRI demonstrates that it is necessary to start the process from the catalyst bed initially filled with a liquid phase to perform an exothermic multiphase catalytic reaction under safe conditions. A completely filled initial state of the catalyst bed provides a moderate temperature of the bed and an existence of less dry pellets, and, as a result, a stationary performance of a reaction in the gaseous phase.

In the experiment presented in Fig. 5, transverse 2D images of the catalyst bed, in the upper (a), middle (b) and lower (c) parts, have been subsequently detected. The intensity scale is the same as in Fig. 3. The rate of a flow of hydrogen heated to 80 °C was

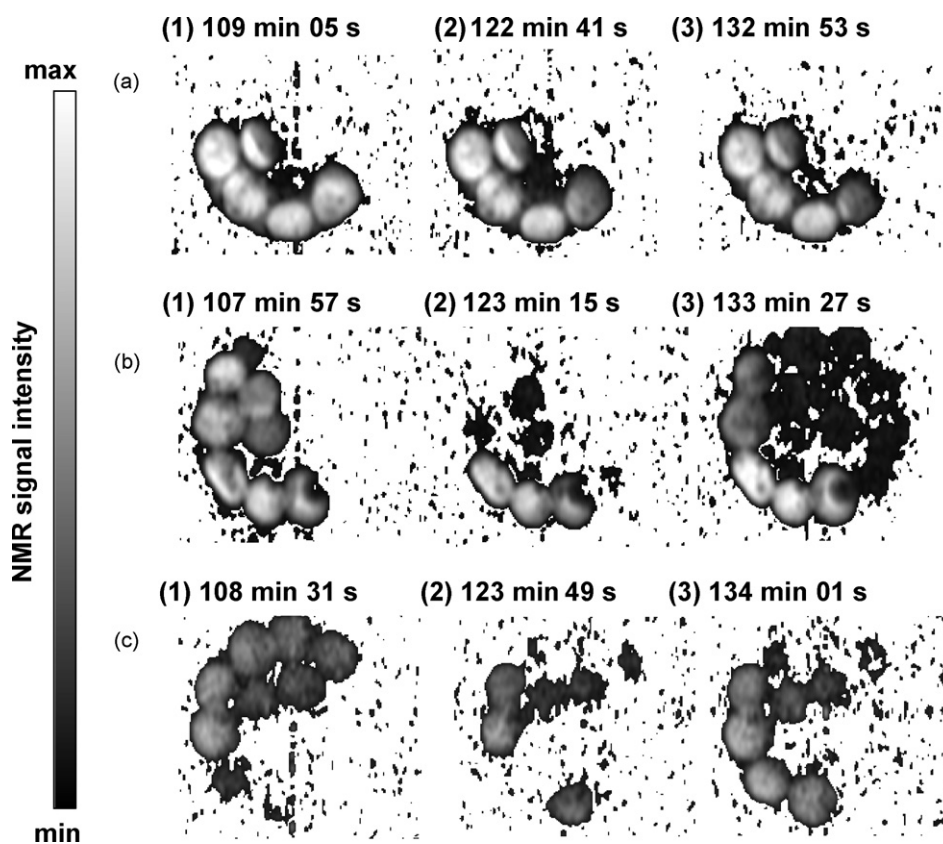


Fig. 5. 2D images of the liquid phase distribution in the catalyst bed of 2–3 mm 1% Pd/ γ -Al₂O₃ pellets in the course of AMS hydrogenation. (a) Upper part of the bed; (b) middle part of the bed; (c) lower part of the bed. The rate of liquid AMS supply was: (1) 3.53×10^{-1} g/s; (2) 2.68×10^{-2} g/s; (3) 3.52×10^{-1} g/s. Time corresponding to the middle of the acquisition period is shown in each image. The change of image intensity from dark grey to light grey corresponds to the increase of the liquid phase content, whereas in the zones of white color the NMR signal intensity is lower than the noise level.

20 cm³/s, the rate of liquid AMS supply was varied during the experiment. When the rate of liquid AMS supply was decreased from 3.53×10^{-2} g/s (Fig. 5(1)) to 2.68×10^{-2} g/s (Fig. 5(2)), the liquid phase distribution in the upper part of the catalyst bed did not change but it resulted in an essential decrease of the liquid phase content in the middle and lower parts of the catalyst bed. Then the rate of a liquid AMS supply has been returned to 3.52×10^{-1} g/s (Fig. 5(3)). It did not influence again the liquid phase distribution in the upper part of the catalyst bed but has resulted in an increase of the liquid phase content in the middle and lower parts of the catalyst bed. The results presented here demonstrate that the distribution of a liquid phase in the part of the catalyst bed close to the reagent inlet is not sensitive to the variation of the rate of a liquid reagent supply. Moving away from the inlet of the catalyst bed, the liquid phase distribution in the catalyst bed becomes more sensitive to the parameter variation.

To establish the state of the individual catalyst pellets comprising the granular bed, the next set of experiments has been carried out on the catalyst bed of 4.2 mm 1% Pd/ γ -Al₂O₃ pellets. Because the inner diameter of a reactor was 10 mm, a nearly regular packing of the catalyst pellets in the bed (three or four pellets in a layer) could be arranged.

Fig. 6 presents the transverse 2D images of the liquid phase distribution in the catalyst bed operating at the temperature of hydrogen flow of 91 °C, the rate of H₂ flow of 39.7 cm³/s. The intensity scale is the same as in Fig. 3. The rate of liquid AMS supply was varied in the course of the experiment. When the first image has been detected, the rate of liquid AMS supply to the bed was 4.09×10^{-1} g/s, and all pellets seen in the image

were filled with a liquid phase. A twofold decrease of the rate of liquid AMS supply did not result in the change of the liquid phase distribution in the catalyst bed (image 2). The further decrease of the rate of liquid AMS supply has resulted in the ignition of one of the catalyst pellets (image 3). A decrease of the rate of liquid AMS supply further by almost a factor of 4 (to 3.23×10^{-2} g/s) has resulted in the ignition and drying of one more catalyst pellet (image 4). Then the liquid AMS supply was turned off that resulted in a complete drying of the catalyst bed. After this, a liquid AMS with the same flow rate as during the detection of the fourth image was supplied to the dry catalyst bed (image 5). It can be seen that again only two pellets are filled with a liquid phase. When the rate of a liquid AMS supply was increased to 2.21×10^{-1} g/s, one more pellet became filled with a liquid phase (image 6).

Therefore, the results presented in Fig. 6 demonstrate that the possibility of ignition of individual catalyst pellets within the catalyst bed in the course of an exothermic multiphase reaction can be realized. These results also show that dry pellets appearing within the catalyst bed as a result of ignition can remain dry despite of an increase of the rate of a liquid reagent supply into the reactor, apparently because of the realization of an exothermic vapor phase reaction in the porous structure of dry pellets.

The next experiment, in which transverse 2D images of the liquid phase distribution in two layers of the catalyst pellets, in the upper and in the lower parts of the catalyst bed, have been detected, has revealed the existence of dry pellets in the trickle bed (Fig. 7a) and dry pellets supplied with a liquid reagent via mechanism of capillary absorption of the liquid phase from

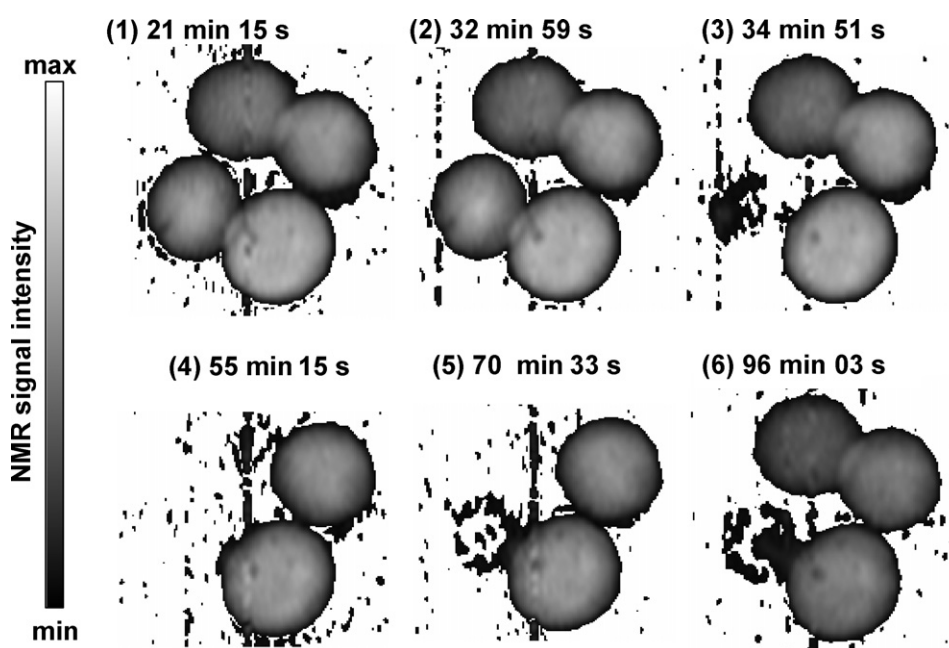


Fig. 6. 2D images of the liquid phase distribution in the catalyst bed of 4.2 mm 1% Pd/ γ -Al₂O₃ pellets in the course of AMS hydrogenation. The rate of liquid AMS supply was: (1) 4.09×10^{-1} g/s, (2) 2.07×10^{-1} g/s, (3) 1.13×10^{-1} g/s, (4) 3.23×10^{-2} g/s, (5) 3.41×10^{-2} g/s (but liquid AMS was supplied to the dry bed), (6) 2.21×10^{-1} g/s. Time corresponding to the middle of the acquisition period is shown in each image. The change of the image intensity from dark grey to light grey corresponds to the increase of the liquid phase content, whereas in the zones of white color the NMR signal intensity is lower than the noise level.

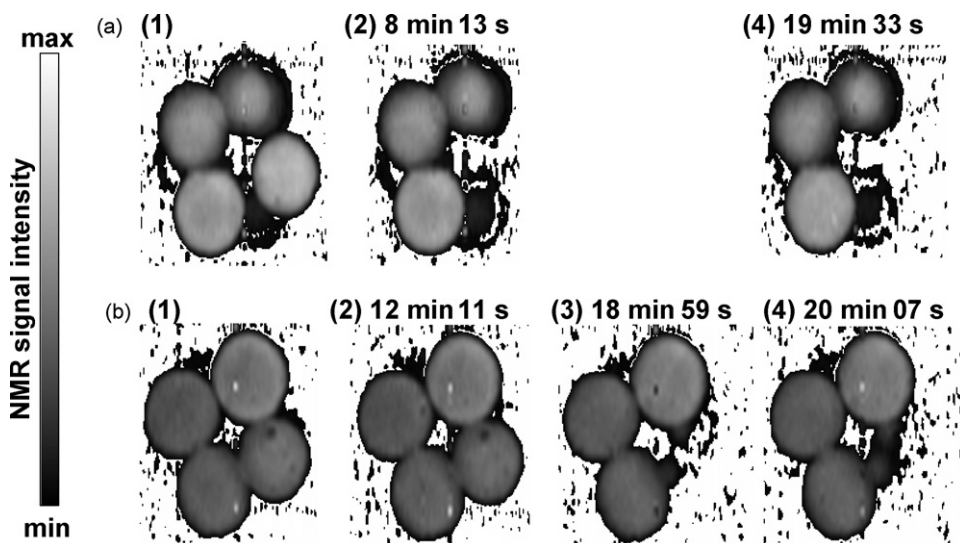


Fig. 7. 2D images of the liquid phase distribution in the catalyst bed of 4.2 mm 1% Pd/ γ -Al₂O₃ pellets in the course of AMS hydrogenation. (a) Upper part of the bed; (b) lower part of the bed. (1) The bed was filled with AMS, the liquid AMS supply was 2.65×10^{-1} g/s, no hydrogen; (2–4) the temperature of hydrogen flow was 85 °C, the rate of H₂ flow was 20 cm³/s, the liquid AMS supply was 2.65×10^{-1} g/s; (2) the liquid AMS supply was turned on to the initially wetted catalyst bed; (3, 4) the liquid AMS supply was turned on to the dry bed. Time corresponding to the middle of acquisition period is shown in each image. The change of the image intensity from dark grey to light grey corresponds to the increase of the liquid phase content, whereas in the zones of white color the NMR signal intensity is lower than the noise level.

the adjoining wetted pellets (Fig. 7b). The reagent absorbed in such a way rapidly evaporates and reacts in the gaseous phase. Thus, such dry pellets operate as “microreactors” based on the principal of reactive evaporation [5] and provide the effective performance of a reaction in the gaseous phase.

A degree of wetting of inner porous structure of pellets when an exothermic reaction is carried out in a multiphase reactor is a very important factor determining productivity of such reactors. There is evidence that pellets not fully wetted with a liquid phase can be found in the trickle bed [6–12]. It is possible to establish a degree of wetting of external surface of pellets by visual observations [13]. A degree of wetting of inner porous structure of pellets in the trickle bed could be estimated from the visually observed degree of wetting of external surface of pellets. A correlation of the degree of wetting of inner porous structure of pellets and a rate of a chemical reaction has been obtained in such a way. It has been established from this correlation that a maximum rate of reaction can be achieved when catalyst pellets are not completely filled with a liquid phase [13,14]. Such method of determining the degree of wetting of inner porous structure seems to be not very reliable. MRI allowed us to visualize directly the inner porous structure of catalyst pellets in the course of an exothermic reaction performed in the trickle bed, as it has been shown above.

For the first time we have observed by an experimental *in situ* method the partially wetted pellets in the operating trickle bed under conditions of occurrence of an exothermic reaction (Fig. 7). The partially wetted catalyst pellets can be hypothetically responsible for the appearance of hot spots in the reactor because an evaporating reagent reacts within such pellets in the gaseous phase leading to an efficient heat generation, temperature rise and corresponding acceleration of the catalytic reaction.

3.3. Application of NMR spectroscopy with spatial resolution to study the reagent and product distribution in an operating gas–liquid–solid catalytic fixed bed reactor

A ¹H NMR signal of the liquid phase without distinguishing the AMS and cumene contributions has been detected to obtain the images shown in Figs. 2–6. NMR spectroscopy is well-known for its ability to distinguish different molecular species and even groups of atoms in a molecule based on the differences in their chemical shifts in NMR spectra. However, the NMR lines of molecules interacting with solid surfaces are broadened in comparison with a homogeneous solution due to the shortening of their nuclear spin relaxation times. This fact complicates the acquisition of spectroscopic information. Nevertheless, an NMR experiment performed with spatial resolution can solve the line width problem. A ¹H NMR spectrum detected for a small volume inside the sample exhibits much narrower and less distorted lines than the one detected for the whole sample, because this volume is much smaller than the characteristic length scale of the magnetic field inhomogeneities, and the quantification of the mixture composition on the basis of NMR spectra becomes possible [4].

On the basis of this fact, a combination of NMR spectroscopy with MRI has been used to visualize the spatial distribution of the reactant-to-product conversion within an operating reactor with a fixed catalyst bed [15]. The stationary regime of the catalyst bed operation (1 mm 1% Pd/ γ -Al₂O₃ pellets) characterized by the rate of hydrogen supply of 10.5 cm³/s, the temperature of gas flow of 79 °C, the rate of a liquid AMS supply of $(9.9\text{--}10.2) \times 10^{-3}$ g/s has been studied. We have carried out a three-dimensional experiment with two spatial and one spectral coordinates. Such experiment allowed us to obtain a two-dimensional image of the liquid phase distribution inside

the trickle bed in the 2 mm thick axial slice, and at the same time to detect a ^1H NMR spectrum in each pixel of the image obtained. As a result, we have obtained the spatially resolved information on the reagent to product conversion by a comparison of the detected ^1H NMR spectra with the spectra of the pure reagent and product. We have observed the tendency of an increase of the product/reagent ratio from top to bottom of the trickle bed and a non-uniformity of the conversion along the radius of the catalyst bed. Very likely, a non-uniformity of the conversion along the radius of the catalyst bed in the reactor operating in the stationary regime under conditions of the liquid reagent and hydrogen supply is caused by a non-uniformity of the liquid reagent flow in the reactor. Further results obtained with a special pulse sequence allowing to detect a 3D image in 30 s have demonstrated the absence of streams of a liquid phase between pellets in the trickle bed even in the case of the maximum rate of liquid reagent supply used in this work. Therefore, we can suppose that flow of a liquid phase in the catalyst bed is realized through the wetted surface of catalyst pellets and capillary flow through inner porous structure of pellets, which is partially confirmed by MRI results (Fig. 7b(3, 4)).

4. Conclusions

MRI has been successfully applied to study *in situ* heterogeneous catalytic reactions carried out in a gas–liquid–solid catalytic fixed bed reactor and to visualize the reaction progress inside a catalyst pellet and a catalyst bed in dynamics, including reactions at elevated temperatures. It has been shown by direct visualization of the spatial distribution of a liquid phase inside the catalyst pellet/bed that the occurrence of an exothermic reaction accompanied by the phase transition “liquid–gas” essentially influences the character of the impregnation of the porous structure with a liquid phase.

It has been shown that under conditions of a reagent evaporation and its vapor-phase hydrogenation the supply of a liquid reagent to the pellet can result in the significant gradients of the liquid phase content inside the catalyst pellet. For the first time the visualization of the non-stationary regime of the catalyst pellet operation characterized by the oscillations of the front of the liquid phase propagation into the pellet and the temperature oscillations has been performed by the direct *in situ* method. The oscillatory behavior of the catalyst pellet operation results from the heat production in the course of an exothermic reaction accompanied by the phase transition.

The character of the liquid phase distribution in the catalyst bed in the course of a hydrogenation reaction under different conditions of the reagent supply has been studied. The essential differences in the liquid phase distribution in the catalyst bed have been revealed when a liquid reagent was supplied to the dry and to the wetted catalyst bed. The existence of the partially wetted catalyst pellets in the catalyst bed which can be hypothetically responsible for the appearance of hot spots in the reactor has been revealed by MRI.

The possibility to apply the NMR spectroscopy with spatial resolution to study the reagent and product distribution in the catalyst bed in an operating gas–liquid–solid catalytic fixed

bed reactor has been shown. The spatially resolved information about the reagent to product conversion for the catalyst bed operating in the stationary regime under conditions of the liquid reagent and hydrogen supply has been obtained in the reaction of AMS hydrogenation. The tendency of an increase of the product/reactant ratio from top to bottom of the catalyst bed as well as a non-uniformity of the conversion along the radius of the bed has been revealed.

The results described above allow us to conclude that the MRI based strategies can be extremely useful for non-invasive visualization of processes taking place in an operating gas–liquid–solid catalytic fixed bed reactor.

Acknowledgements

This work was supported by the grants from RFBR (05-03-32472), CRDF (RU-C1-2581-NO-04; RUP1-2667-NO-05), the Global Energy Foundation, SB RAS (integration grant 11) and the Russian President's program of support of the leading scientific schools (NSch-4821.2006.3). A.A. Lysova thanks the Russian Science Support Foundation for financial support.

References

- [1] P.T. Callaghan, Principles of Nuclear Magnetic Resonance Microscopy, Clarendon Press, Oxford, 1991.
- [2] I.V. Koptuyug, R.Z. Sagdeev, Modern applications of NMR tomography in physical chemistry. The characteristic features of the technique and its applications to studies of liquid-containing objects, Russ. Chem. Rev. 71 (2002) 593–617.
- [3] I.V. Koptuyug, R.Z. Sagdeev, Non-traditional applications of NMR tomography, Russ. Chem. Rev. 72 (2003) 165–191.
- [4] I.V. Koptuyug, A.V. Kulikov, A.A. Lysova, V.A. Kirillov, V.N. Parmon, R.Z. Sagdeev, NMR imaging of the distribution of the liquid phase in a catalyst pellet during α -methylstyrene evaporation and its vapor-phase hydrogenation, JACS 124 (2002) 9684–9685.
- [5] N.A. Kuzin, A.V. Kulikov, A.B. Shigarov, V.A. Kirillov, A new concept reactor for hydrocarbon hydrogenation in the reactive evaporation mode, Catal. Today 79–80 (2003) 105–111.
- [6] A.H. Germain, A.G. Lefebvre, G.A. L'Homme, Experimental study of catalytic trickle bed reactor, Adv. Chem. Ser. 133 (1974) 164–180.
- [7] J.C. Charpentier, Recent progress in two-phase gas–liquid mass transfer in packed beds, Chem. Eng. J. 11 (1976) 161–181.
- [8] M. Hartman, R.W. Coughlin, Oxidation of SO_2 in a trickle-bed reactor packed with carbon, Chem. Eng. Sci. 27 (1972) 867–880.
- [9] C.N. Satterfield, F. Ozel, Direct solid-catalyzed reaction of a vapor in an apparently completely wetted trickle-bed reactor, AIChE J. 19 (1973) 1259–1261.
- [10] W. Sedriks, C.N. Kenney, Partial wetting in trickle bed reactors, Adv. Chem. Ser. 109 (1972) 251–255.
- [11] J. Hanika, K. Sporka, V. Ruzicka, J. Hrstka, Measurement of axial temperature profiles in an adiabatic trickle bed reactor, Chem. Eng. J. 12 (1976) 193–197.
- [12] S. Morita, J.M. Smith, Mass transfer and contacting efficiency in a trickle-bed reactor, Ind. Eng. Chem. Fundam. 17 (1978) 113–120.
- [13] G.A. Funk, M.P. Harold, K.M. Ng, Experimental study of reaction in a partially wetted catalytic pellet, AIChE J. 37 (1991) 202–214.
- [14] M. Herskowitz, R.G. Carbonell, J.M. Smith, Effectiveness factors and mass transfer in trickle-bed reactors, AIChE J. 25 (1979) 272–283.
- [15] I.V. Koptuyug, A.A. Lysova, V.A. Kirillov, A.V. Kulikov, V.N. Parmon, R.Z. Sagdeev, Functional imaging and NMR spectroscopy of an operating gas–liquid–solid catalytic reactor, Appl. Catal. A: Gen. 267 (2004) 143–148.